

MINISTRY OF EDUCATION
AND TRAINING

VIETNAM ACADEMY OF
SCIENCE AND TECHNOLOGY
GRADUATE UNIVERSITY OF SCIENCE AND TECHNOLOGY



DAO PHI HUNG

**STUDY ON PREPARATION, STRUCTURAL CHARACTERISTIC,
PROPERTIES OF MULTILAYER COATINGS BASED ON
ACRYLIC EMULSION POLYMERS AND NANOFILLERS**

SUMMARY OF DISSERTATION ON ORGANIC CHEMISTRY
Code: 9 44 01 14

Ha Noi, 2023

The dissertation is completed at: Graduate University of Science and Technology, Vietnam Academy Science and Technology

Supervisor: Prof. Dr. Thai Hoang, Institute for Tropical Technology.

Referee 1: Prof. Dr. Dinh Thi Ngo

Referee 2: Assoc. Prof. Dr. Nguyen Quang Tung

Referee 3: Assoc. Prof. Dr. Nguyen Minh Ngoc

The dissertation will be examined by Examination Board of Graduate University of Science and Technology, Vietnam Academy of Science and Technology at 9h00, 04 Dec. 2023

The dissertation can be found at:

- Graduate University of Science and Technology Library.
- National Library of Vietnam.

INTRODUCTION

1. The urgency of the thesis

Global warming has led to an increased demand for cooling energy in buildings. In the context of climate change adaptation and mitigation, many countries worldwide are concerned about reducing CO₂ emissions and enhancing energy security. As a result, there has been growing interest in researching and developing solar reflective paints (SRP) for buildings. The lifespan of paint coatings significantly depends on the development of microorganisms (bacteria, yeast, and mold) on the paint's surface. Consequently, there is a need for paint systems that can inhibit the growth of these microorganisms to extend the coating's lifespan. Moreover, antibacterial paint coatings have been investigated for their potential to reduce the risk of microbial infections. Currently, the research, development, and refinement of solar reflective and antibacterial coatings represent a research direction with practical importance, relevance, and significant scientific value.

Paints using waterborne binders not only reduce volatile organic compounds but also enhance fire safety during manufacturing and transportation. Acrylic emulsion polymers are a popular type of waterborne binder. Paint formulas based on acrylic emulsion polymers, with reasonable costs, can produce coatings with excellent weather durability, chemical resistance, and minimal environmental impact. Consequently, the PhD candidate has chosen the project: "Study on the preparation, structural characteristics, and properties of multifunctional coatings based on acrylic emulsion polymers and nanofillers."

2. Objectives of the thesis

Fabrication a coating based on acrylic emulsion polymers with nanofillers and organic additives that exhibit both solar-reflective and antimicrobial properties with several specific objectives:

- Modified R-TiO₂, ZrO₂ nanoparticles (NPs) with suitable organic coupling agents with the aim of achieving regular dispersion within the acrylic emulsion polymer matrix.

- Evaluate the synergistic effects of organically modified nanofillers on the properties of acrylic coatings, including mechanical properties, thermal stability, and solar reflection. Additionally, assess the synergistic effects of both organic

and inorganic antibacterial agents on the antimicrobial properties of the coating.

3. Content of the thesis

The thesis includes:

- R-TiO₂ NPs were modified with two coupling agents, namely [3-(methacryloyloxy)propyl]trimethoxy-silane (TMSPM) and isopropyl tri(dioctylpyrophosphate)titanate (KR12). Similarly, ZrO₂ NPs were also modified with TMSPM, KR12 and (3-glycidyloxypropyl)triethoxy-silane (GPTES). The primary objectives were to determine the characteristics, properties, and morphology of these modified NPs. Following this, several properties of coatings based on acrylic emulsion polymers and these modified NPs were assessed.

- Effect of modified NPs on properties of nanocomposite coatings, including solar reflection, cooling performance, water permeability and morphology was determined.

- The antimicrobial ability of the acrylic coating was assessed with regard to the impact of Ag-Zn/zeolite and 2-n-octyl-4-isothiazolin-3-one (OIT).

4. Layout of the thesis

The thesis comprises 120 pages, with 53 figures, 40 tables, and a bibliography of 114 references. The structure of the thesis follows a typical layout, which includes an introduction, three content chapters, and a conclusion. Notably, the novelty of the research has resulted in the publication of six papers, with four papers listed in SCIE journals and two in Scopus-indexed journals, as well as a granted patent.

CHATER 1. OVERVIEW

Chapter 1 consists of 26 pages and includes 15 figures and 4 tables. This chapter provides an introduction to the current state of research and development in acrylic emulsion polymers, with a focus on enhancing their properties and applications. The chapter discusses a simple yet highly efficient approach, which involves incorporating metal oxide NPs into acrylic emulsion polymers. This chapter also presented the principal of NPs modified with silane/titanate coupling agents.

Chapter 1 also provides an overview of the current state of research and development in organic coatings that possess excellent solar reflection and antimicrobial properties. The overview reveals that multifunctional and

environmentally friendly coatings, which include properties like solar reflection, high thermal stability, good weather resistance, strong antimicrobial abilities, and low volatile organic compounds, have not received as much attention with relatively low publication output. The published works primarily focused on the individual effects of separate agents on coating properties. Solar-reflective and antibacterial coatings were traditionally prepared using separate agents, such as nanofillers or organic antibacterial additives. However, there has been a growing emphasis on the incorporation of both organic and inorganic additives. As a result, the study of the preparation and application of coatings based on acrylic emulsion polymers with nanofillers and antimicrobial additives has significantly expanded the possibilities for acrylic emulsion polymers. Furthermore, these coatings play a vital role in reducing cooling energy consumption and enhancing the aesthetics of buildings.

CHAPTER 2. EXPERIMENTAL

Chapter 2 is presented in 13 pages, 4 figures and 5 tables which includes:

2.1. Materials

2.2. Modified NPs preparation

2.3. Acrylic nanocomposite coating preparation

2.4. Solar reflective paint preparation

2.5. Analysis

2.5.1. Determination of characteristics, properties of modified NPs

The characteristics and properties of the modified NPs were analyzed using various physical analytical instruments, available at the Vietnam Academy of Science and Technology and Vietnam National University, Hanoi. These instruments included FTIR, TGA, FESEM, XRD, DLS, and UV-Vis-NIR diffuse reflectance spectrometer.

2.5.2. Determination of characteristics and properties of paint coating

The properties of the paint coating, including abrasion resistance, water permeability, weather durability, resistance to microorganisms, and cooling performance, were determined in accordance with appropriate ASTM, ISO, and TCVN standards.

CHAPTER 3. RESULTS AND DISCUSSION

3.1. Study on modification of R-TiO₂ NPs and ZrO₂ NPs

In the thesis, R-TiO₂ and ZrO₂ NPs were modified with TMSPM, KR12

and GPTES with initial content of 3 wt.% (compare to the NPs weight) (coded by mTi3T, mTi3K and mZr3T, mZr3K, mZr3G, respectively). The characteristics and properties of both unmodified R-TiO₂ and ZrO₂ (coded respectively as u-Ti, u-Zr) and organically modified NPs were determined and are presented below.

3.1.1. Characteristics and properties of organically modified R-TiO₂ NPs

3.1.1.1. FTIR analysis

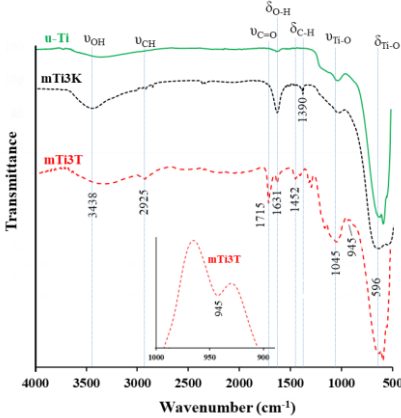


Fig. 3.1. FTIR of u-Ti, mTi3K and mTi3T

In comparison with FTIR of u-Ti, FTIR of mTi3K and mTi3T (Fig. 3.1) has new appearance absorptions at 2925 cm⁻¹ and 1383 cm⁻¹ corresponding to C-H linkages of KR12, TMSPM. Specially, FTIR of mTi3T appears a vibration at 945 cm⁻¹, corresponding to Ti-O-Si linkages. Consequently, the organic modification of R-TiO₂ NPs was successful.

3.1.1.2. Coupling agent content grafted on R-TiO₂ NPs

Table 3.1. Content of coupling agent grafted on R-TiO₂ NPs

Sample	Weight loss at 900°C (%)	The maximum thermal degradation (°C)	Molecular weight of agent (au)	Content of agent grafted on NPs surface	
				(mmol/g)	mg/g
u-Ti	0,62	277	-	-	-
mTi3K	0,75	304	1311	10 ⁻³	1,3
mTi3T	3,6	322	248	0,122	29,8

Based on TGA diagrams, content of agent grafted on NPs surface can be calculated as follow formula:

$$\text{Grafted content} \left(\frac{\text{mmol}}{\text{g}} \right) = \frac{\Delta m \cdot 10^3}{(100 - \Delta m) \cdot M_{\text{agent}}} \quad (1)$$

In there: Δm is weight loss of sample in temperature range of 100-900°C, M_{agent} is molecular weight of agent.

As can be seen from Table 3.1, although R-TiO₂ NPs were modified with the same initial content of TMSPM and KR12, the content of TMSPM grafted onto the NPs is higher. The reason may be the variance in size of the functional groups, which can influence the hydrolysis and condensation reactions.

3.1.1.3. Morphology

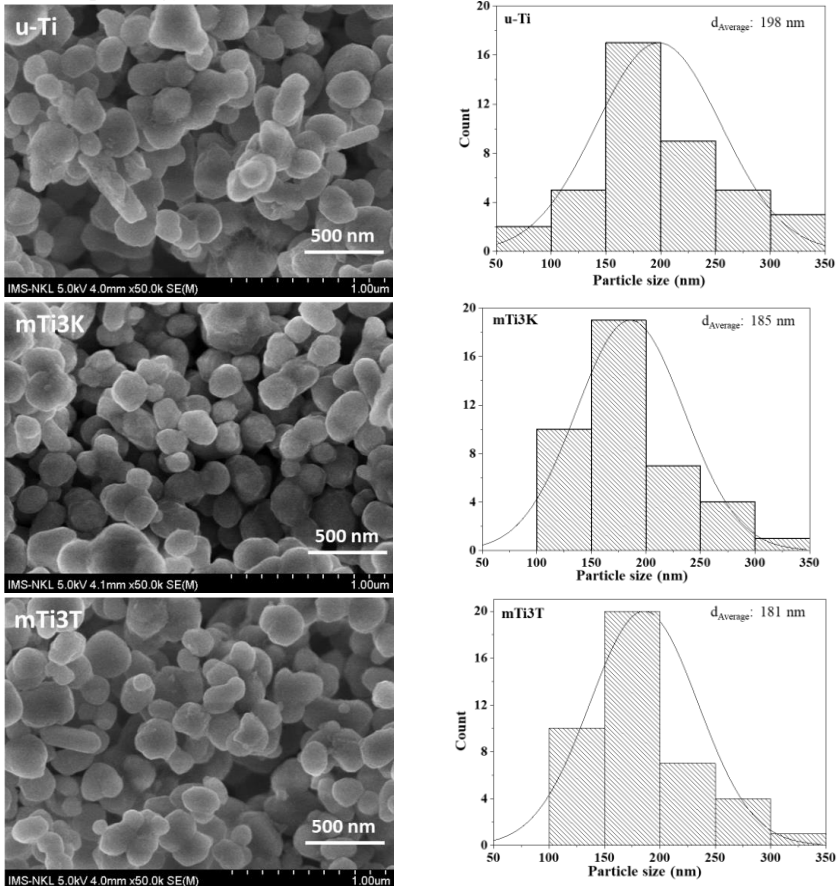


Fig. 3.2. FESEM image and corresponding size distribution of u-Ti, mTi3T and mTi3K

Fig. 3.2. indicated that organic modification can reduced the agglomeration of nanopartilces but not affected to mophorlogy of NPs.

3.1.1.4. Size distribution analysis

As depicted in Figure 3.3, the modified R-TiO₂ NPs exhibit better dispersion ability in water compared to u-Ti.

The mTi3T NPs exhibit the best dispersion. Consequently, mTi3T was chosen for further studies.

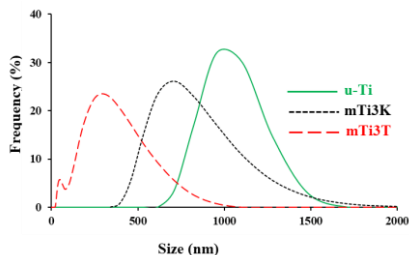


Fig. 3.3. Size distribution diagrams of u-Ti, mTi3T and mTi3K

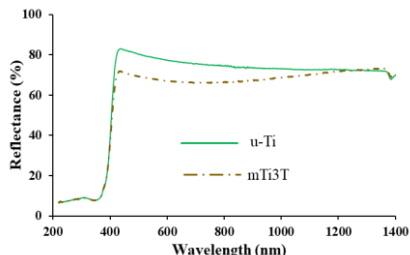


Fig. 3.4. UV-Vis-NIR spectra of u-Ti and mTi3T

3.1.1.5. UV-Vis-NIR diffuse reflectance spectroscopy analysis

The light reflection ability of mTi3T NPs is insignificantly lower than that of u-Ti NPs (Fig. 3.4).

3.1.1.6. XRD patterns analysis

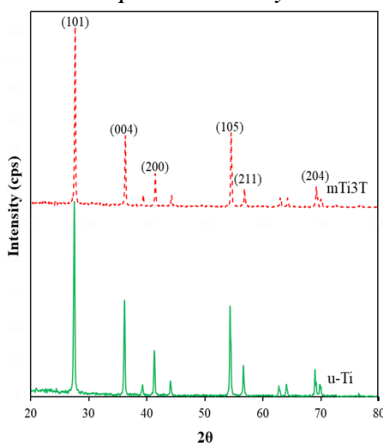


Fig. 3.5. XRD patterns of u-Ti and mTi3T

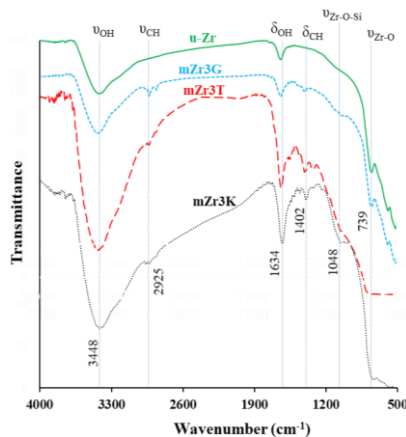


Fig. 3.6. FTIR spectra of u-Zr, mZr3K, mZr3T and mZr3G

No difference is observed between the XRD patterns of u-Ti and mTi3T NPs (see Fig. 3.5). This result demonstrates that the organic modification of the R-TiO₂ NPs surface does not alter the crystal structure of the R-TiO₂ NPs.
mTi3T have better dispersion and stability in comparison with mTi3K.

Thus, *mTi3T* have been chosen for further studies.

3.1.2. Characteristics and properties of organically modified ZrO_2 NPs

3.1.2.1. FTIR analysis

In contrast to the FTIR spectrum of u-Zr NPs (Figure 3.6), the FTIR spectrum of organically modified ZrO_2 exhibits distinct absorption peaks corresponding to the C-H bonds present in the organic modifying agents. Notably, in the spectra of *mZr3T* and *mZr3G*, an additional absorption peak at 1048 cm^{-1} is evident, indicating the presence of the characteristic Zr-O-Si bond. This observation provides conclusive evidence of the successful modification of ZrO_2 NPs by organic agents.

3.1.2.2. Coupling agent content grafted on ZrO_2 NPs

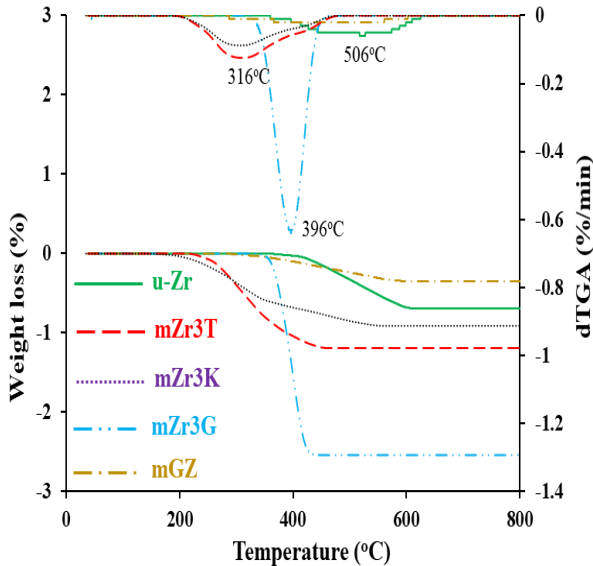


Fig. 3.7. TGA and dTGA diagrams of u-Zr, *mZr3K*, *mZr3T*, *mZr3G* and mixture of hydrolyzed GPTES with ZrO_2 (*mGZ*)

By assessing the mass loss of ZrO_2 NPs before and after modification, the amount of grafting agent on the surface of ZrO_2 NPs can be calculated using the formula provided in Section 3.1.1.2 (refer to Table 3.3). It is evident that the content of GPTES agent grafted onto the NPs surface is the highest due to the characteristics of functional groups.

The similarity in the TGA diagram shapes between *mGZ* and u-Zr NPs (Fig. 3.7) is evident, indicating that without heating, no dehydration reaction occurs between the OH group of the silanol and the OH group on the NPs surface. Furthermore, the silanols not involved in the grafting reaction on the NPs surface have been effectively washed off.

Fig. 3.2. Content of coupling agent grafted on ZrO₂ NPs

Sample	Weight loss at 900°C (%)	The maximum thermal degradation (°C)	Molecular weight of agent (au)	Content of agent grafted on NPs surface	
				(mmol/g)	(mg/g)
u-Zr	0,69	506	-	-	-
mZr3K	0,91	308	1311	$1,6 \cdot 10^{-3}$	2,1
mZr3T	1,19	316	248	0,02	5,0
mZr3G	2,54	396	278	0,068	18,9

3.1.2.3. Morphology

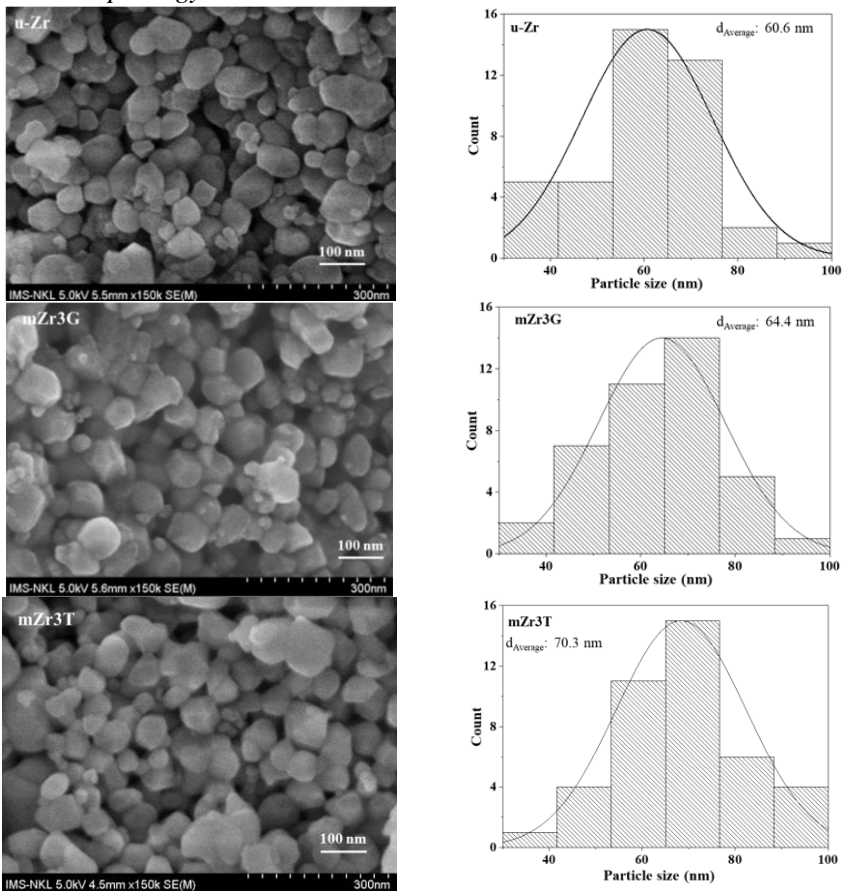


Fig. 3.8. FESEM images and corresponding to distribution size of u-Zr, mZr3T, mZr3K and mZr3G

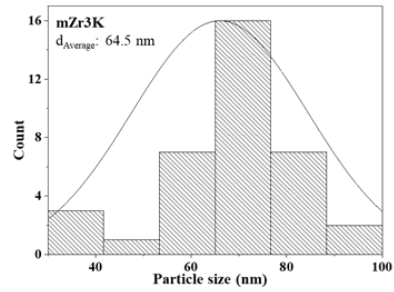
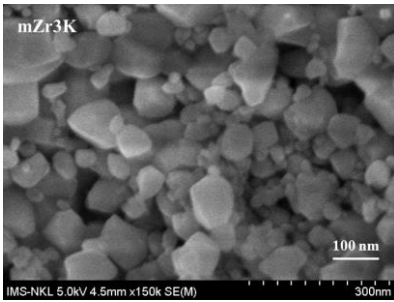


Fig. 3.8. (continued) FESEM images and corresponding to distribution size of mZr3K

As can be observed in Fig. 3.8, the organic modification increased the size of ZrO₂ NPs but not affected to morphology of these NPs.

3.1.2.4. Size distribution analysis

As can be seen from Fig. 3.9, modified ZrO₂ NPs has better dispersion in water than u-Zr NPs. The mZr3G exhibited the best performance, and thus choosing for further studies.

3.1.2.5. UV-Vis-NIR diffuse reflectance spectroscopy analysis

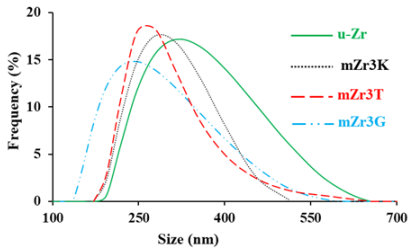


Fig. 3.9. Size distribution diagrams of u-Zr, mZr3T, mZr3K and mZr3G

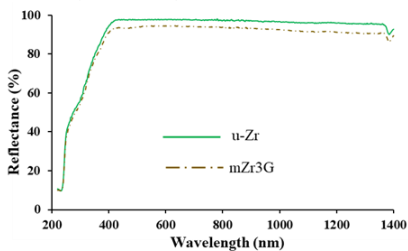


Fig. 3.11. UV-Vis-NIR spectra of u-Zr and mZr3G

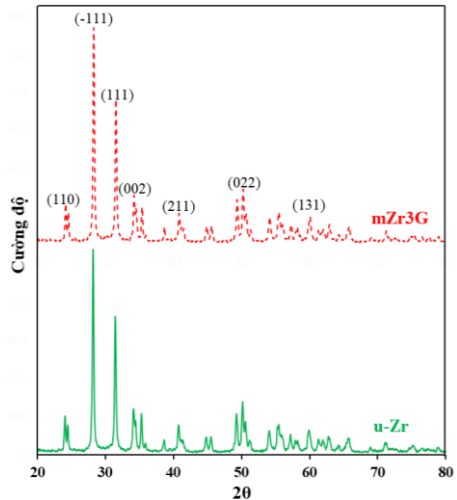


Fig. 3.10. XRD patterns of u-Zr NPs and mZr3G NPs

As can be seen from Fig. 3.10, the diffuse reflectance of mZr3G NPs was

insignificantly lower than that of u-Zr NPs.

3.1.2.6. XRD pattern analysis

Comparing the XRD patterns of u-Zr and mZr3G NPs, as shown in Fig. 3.13, reveals that there is no difference between the two XRD patterns of u-Zr and mZr3G NPs.

3.2. Characteristics and properties of acrylic nanocomposite coating

3.2.1. Effect of modified R-TiO₂ NPs on acrylic coating's properties

The properties of nanocomposite coatings largely depend on the dispersion ability and NPs content. In this study, the falling abrasion resistance test was employed to determine the suitable modifier content and the appropriate content of organically modified NPs.

3.2.1.1. Effect of coupling agent content

Table 3.3. Abrasion resistance of acrylic coating with various nanofillers.

Sample	Abrasion resistance (L/mil)	one way ANOVA
A0	84 ± 3.35	<i>F</i> : 287,8 <i>p</i> _{value} : 8,1.10 ⁻²⁴
AuT	135 ± 3.83	
A2mTi1T	174 ± 4.24	
A2mTi3T	187 ± 6.62	
A2mTi5T	142 ± 3.25	
A2mTi10T	128 ± 2.33	
A2mTi20T	125 ± 2.86	

The results of abrasion resistance of coatings filled with 2 wt.% R-TiO₂ NPs which were modified with different TMSPM content (mTi_xT, with x = 1, 3, 5, 10 and 20 wt.% TMSPM compared to R-TiO₂ NPs) indicated that A2mTi3T coating has the highest value. Thus, mTi3T NPs have been chosen for further studies.

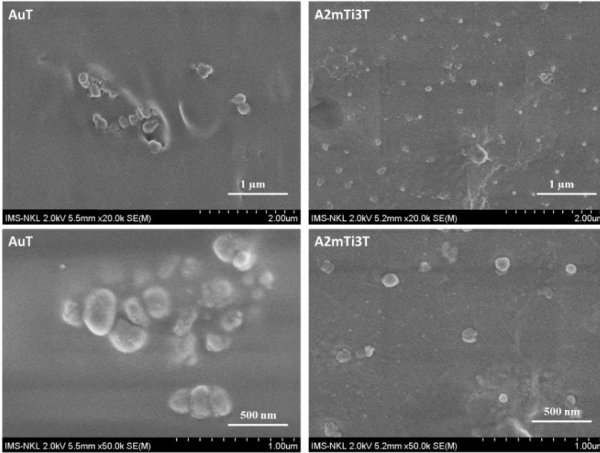
3.2.1.2. Effect of mTi3T content on properties of acrylic coating

Table 3.4. Abrasion resistance of acrylic coating with various mTi3T content

Sample	Abrasion resistance (L/mil)	Oneway ANOVA
A0.5mTi3T	158 ± 2.88	<i>F</i> = 23,1 <i>p</i> _{value} = 4,6. 10 ⁻²⁴
A1mTi3T	173 ± 5.08	
A2mTi3T	187 ± 6.62	
A4mTi3T	173 ± 4.46	

The obtained results of abrasion resistance of coating filled with various mTi3T NPs content (được ký hiệu AxmTi3T, with x=0.5, 1, 2 và 4 wt.% of mTi3T) (Table 3.4) shows that A2Ti3T has the highest value and has been chosen for further studies.

3.2.1.3. Morphology



As depicted from FESEM images (Fig. 3.13), u-Ti NPs agglomerated to big cluster in AuT coating while mTi3T NPs exhibit the good dispersion in A2mTi3T coating.

Fig. 3.12. FESEM images of AuT and A2mTi3T coating

3.2.2. Effect of organically modified ZrO₂ NPs on acrylic coating's properties

3.2.2.1. Effect of coupling agent content

The results of abrasion resistance of coating filled with 2 wt.% nano ZrO₂ modified with different content of GPTES (mZrxG, with x = 1, 3, 5, 10 and 20 wt.% GPTES compared to nano ZrO₂) showed that the coating filled with mZr3G NPs had highest value and thus mZr3G NPs have been chosen for further studies (Table 3.5).

Table 3.5. Abrasion resistance of acrylic coating with various nanofillers

Sample	Abrasion resistance (L/mil)	Oneway ANOVA
A0	84 ± 3.35	F = 316, p = 2,2.10 ⁻²⁴
AuZ	77 ± 2.64	
A2mZr1G	156 ± 3.4	
A2mZr3G	174 ± 3.6	
A2mZr5G	155 ± 7.1	
A2mZr10G	151 ± 5.7	
A2mZr20G	150 ± 6.9	

3.2.2.2. Effect of mZr3G content on properties of acrylic coating

Effect of mZr3G NPs content on abrasion resistance of acrylic coating has been determined. The obtained results indicated A2mZr3G reaches the highest value, 174 L/mil, and has been chosen for further studies.

Table 3.6. Abrasion resistance of acrylic coating with various mZr3G content

Sample	Abrasion resistance (L/mil)	Oneway ANOVA
A0.5mZr3G	142 ± 4.92	F = 24, p _{value} = 1,66.10 ⁻⁷
A1mZr3G	152 ± 5.69	
A2mZr3G	174 ± 3.6	
A3mZr3G	172 ± 7.52	
A5mZr3G	156 ± 6.9	

3.2.2.3. Morphology of acrylic coating filled with ZrO₂ NPs

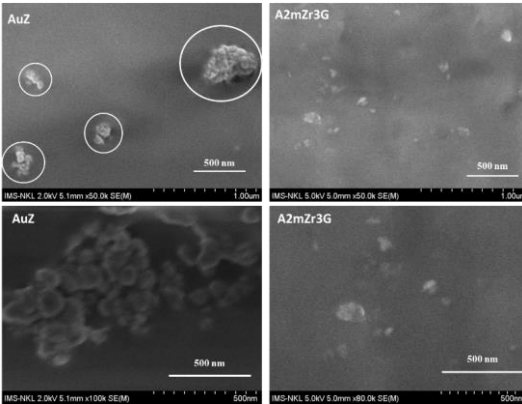


Fig. 3.13. FESEM images of AuZ and A2mZr3G

he FESEM image (Figure 3.15) illustrates that the AuZ coating comprises u-Zr NPs agglomerate to form larger-sized particles. In contrast, the mZr3G NPs exhibit a relatively uniform dispersion in A2mZr3G. This reduction in agglomeration is a key factor contributing to the significantly enhanced abrasion resistance observed in the A2mZr3G coating compared to the A0 coating.

3.2.3. Effect of mZr3G NPs and mTi3T NPs on acrylic coating's properties

3.2.3.1. Effect of mZr3G and mTi3T NPs on coating abrasion resistance

The study examines the impact of the mTi3T/mZr3G ratio (specifically, mTi3T/mZr3G = 2/0, 1.5/0.5, 1/1, 0.5/1.5, and 0/2 were coded as A2mTi3T, A15TZ, A1TZ, AT15Z and A2mZr3G) on the abrasion resistance of acrylic coating (refer to Table 3.7). The obtained results indicated that the A1TZ and A15TZ coatings have the highest value and have been selected for further studies.

Table 3.7. Abrasion resistance of acrylic coating filled with various weight ratio of mZr3G and mTi3T

Sample	Abrasion resistance (L/mil)	Oneway ANOVA
A2mTi3T	187 ± 6.62	F = 18,03 p _{value} = 10 ⁻⁴
A15TZ	188 ± 3.33	
A1TZ	199 ± 3.78	
AT15Z	181 ± 3.14	
A2mZr3G	172 ± 7.52	

3.2.3.2. Effect of mZr3G and mTi3T NPs on acrylic coating's light diffuse reflectance

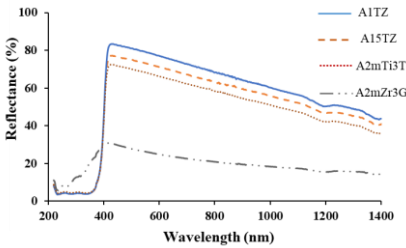


Fig. 3.14. UV-Vis-NIR spectra of acrylic coatings filled with various weight ratio of mZr3G and mTi3T

The coating incorporating both mTi3T and mZr3G NPs concurrently exhibits superior efficiency in diffuse radiation reflection compared to the film containing only one type of NPs. This heightened efficiency is attributed to the resonance effect and interaction between R-TiO₂ and ZrO₂ NPs (Fig. 3.14). Notably, the A1TZ coating demonstrates the highest light reflection capability, suggesting its suitability for further studies.

3.2.3.3. Effect of mZr3G and mTi3T NPs on acrylic coating's thermal stability

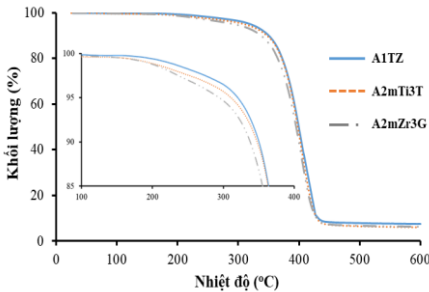


Fig. 3.15. TGA diagrams of acrylic coatings filled with various weight ratio of mZr3G and mTi3T

The TGA diagram (Fig. 3.15) reveals that the A1TZ coating has the highest onset temperature of mass loss compared to other coatings. The reason lies in the synergistic effect, the interaction between R-TiO₂ and ZrO₂ NPs, which restricts the impact of temperatures and the penetration of oxygen into the coating.

3.2.3.4. Effect of mZr3G and mTi3T NPs on acrylic coating's weather durability

Accelerated weather testing, also known as artificial weather testing, is an effective method for rapidly predicting the lifespan or durability of polymer coatings. The extent of deterioration or aging in acrylic films can be assessed by monitoring changes in functional group content, primarily through FTIR spectroscopy, and measuring weight loss during the accelerated weather testing.

- FTIR analysis

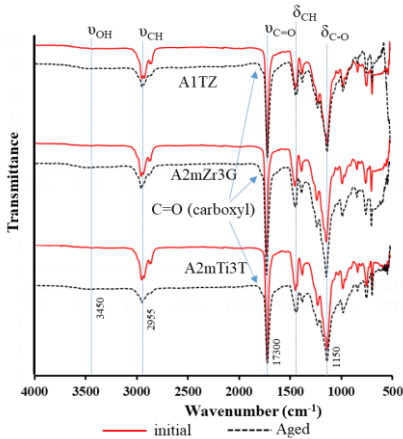


Fig. 3.16. FTIR spectra of acrylic coatings filled with different weight ratios of mZr3G and mTi3T at both the initial stage and after 54 aging cycles

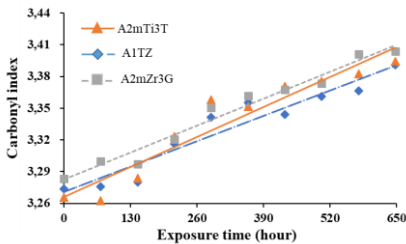


Fig. 3.17. The change of CI of acrylic coatings filled with different weight ratios of mZr3G and mTi3T upon weathering test

FTIR spectrum analysis (Figure 3.18) reveals that the coating, following the accelerated weathering test, displays a new absorption peak at 1780 cm^{-1} , a characteristic of the valence vibration of the C=O bond in the carboxylic acid group. Furthermore, in comparison to the FTIR spectrum of the coating before the accelerated weathering test, alterations in the intensity of absorption peaks have been observed. Specifically, the intensity of the absorptions characteristic of the O-H bond, has increased, while the intensity of the absorption peaks related to the C=O, C-H, and C-O bonds has decreased.

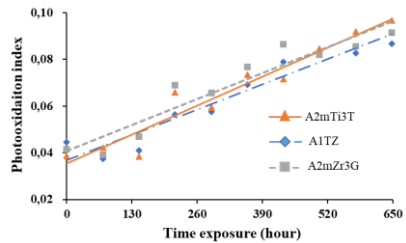


Fig. 3.18. The change of PI of acrylic coatings filled with different weight ratios of mZr3G and mTi3T upon weathering test

In assessing the weather resistance of coatings during weather testing, the carbonyl group index (CI) and photooxidation index (PI) are commonly employed. These indices are calculated based on the intensity of spectral peaks associated with the carbonyl group (1730 cm^{-1}) and the OH group (3450 cm^{-1}) in comparison to the intensity of the C-H group (1450 cm^{-1}).

However, it's important to note that the slopes of the trend lines representing the changes in the CI and PI indices of the coatings differ. Notably, the slope of the trend lines for the CI and PI indices in the A1TZ paint film is the lowest. This signifies that the A1TZ paint film exhibits the highest level of weather resistance among the surveyed acrylic coatings.

- Weight loss of acrylic coatings upon weathering test

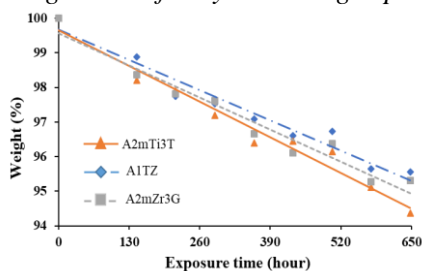


Fig. 3.19. The change of weight loss of acrylic coatings filled with different weight ratios of mZr3G and mTi3T upon weathering test

It is evident that the change in weight loss of the coatings during the accelerated weathering test is relatively small (Fig. 3.19). Even after 54 testing cycles, the weight of the coating has only decreased by approximately 5%. Notably, the slope of the trend line for mass loss in the A1TZ coating is the lowest, indicating that the A1TZ coating boasts the most exceptional weather durability.

Thus, combining mTi3T and mZr3G NPs can create a synergistic effect enhancing the properties of acrylic coatings (abrasion resistance, thermal durability, light diffuse reflection and weather resistance) compared to a coating containing only one specific type of NPs.

3.3. Study on improvement of solar reflective coating properties

3.3.1. Effect of nanoparticles on acrylic coating's solar reflection

Based on the results obtained in section 3.2, the mixture of mTi3T + mZr3G NPs (with a weight ratio of 1/1) was selected for use as an additive in SRP on the base of acrylic emulsion polymer. The effect of the mixture of mTi3T + mZr3G NPs content replacing micro R-TiO₂ particles on the SRP formula was determined using the diffuse reflectance spectrum of coatings, namely SRP0, SRP0.5, SRP1 and SRP2. These coatings have a composition corresponding to the content of the mTi3T + mZr3G nanoparticle mixture used to replace R-TiO₂ microparticles, which are 0%, 0.5%, 1% and 2%, respectively. It can be seen that

replacing micro R-TiO₂ particles with a mixture of mTi3T + mZr3G NPs has contributed to increasing the diffuse reflection light ability of the SRP0 (Fig. 3.20). One of the reasons may be synergistic effect of mTi3T + mZr3G NPs and micro R-TiO₂ particles (Fig. 3.21). SRP1 coating with good reflectivity will be selected for further research.

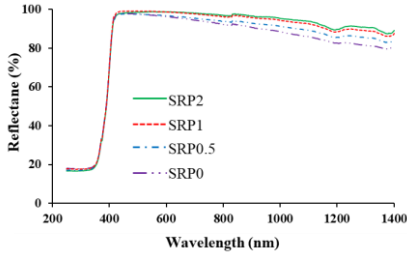


Fig. 3.20. Diffuse reflectance spectra of SRP and paint filled with various content of mixture mTi3T + mZr3G replacing R-TiO₂ microparticles

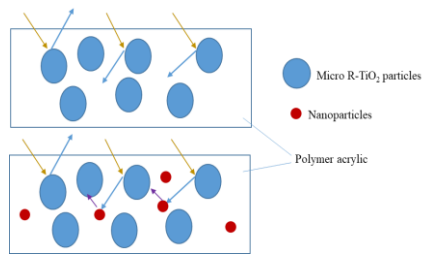


Fig. 3.21. The structure simulates a SRP coating without and with a mixture of organically modified inorganic NPs

3.3.2. Cooling performance of SRP

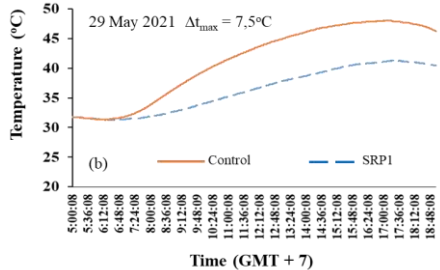
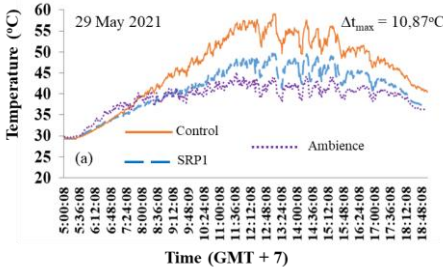


Fig. 3.22. Difference in outside surface temperature (a) and air temperature (b) in the test chamber coated by SRP1 compared to the control chamber

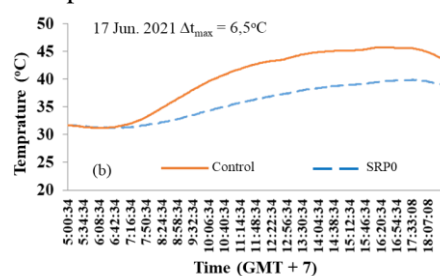
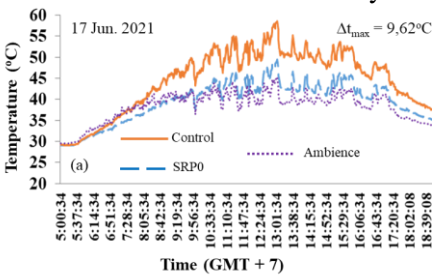


Fig. 3.23. Difference in outside surface temperature (a) and air temperature (b) in the test chamber coated with SRP0 compared to the control chamber

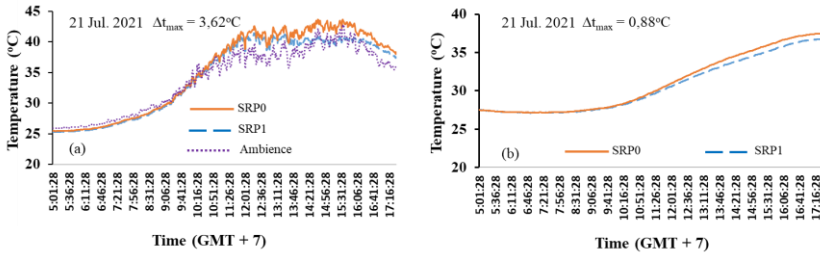


Fig. 3.24. Difference in outside surface temperature (a) and air temperature (b) in the test chamber coated by SRP1 compared to the chamber coated by SRP0

Cooling performance of the solar reflective paint system containing the mTi3T + mZr3G NPs mixture (SRP1) and the comparison to the waterproof paint system (based on acrylic resin combined with cement) has been determined. Changes in the surface temperature of the test chamber and the air temperature in the test chamber of the paint systems are presented in Fig. 3.22 – Fig. 3.24, respectively. It can be seen that when replacing 1% of R-TiO₂ microparticles, it increased the cooling performance.

3.3.3. Water permeability

Table 3.8. Water permeability of SRP0 and SRP1

Sample	Water permeability ($\text{g}\cdot\text{m}^{-2}\cdot\text{h}^{-0.5}$)
SRP0	0.0113 ± 0.0005
SRP1	0.0058 ± 0.0004

It is evident that the water permeability of the SRP1 coating is significantly lower than that of the SRP0 coating (Table 3.8).

3.3.4. Morphology of SRP coatings

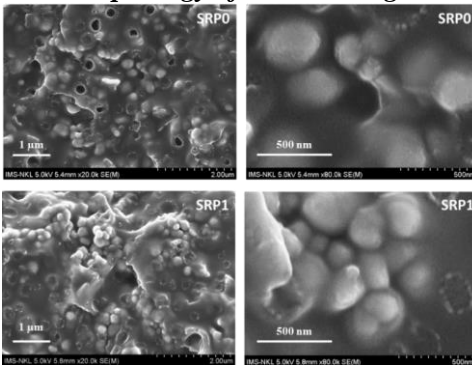


Fig. 3.25. FESEM images of cross section of SRP0 and SRP1

The FESEM images show (Fig. 3.25) that the SRP0 coating is not uniform, with many defects such as gaps and micro-pores. The SRP1 structure is tighter and uniform with less defects. This is the reason why the properties of SRP1 paint film are better than SRP0.

Therefore, the substitution of R-TiO₂ microparticles with mixture of mTi3T + mZr3G NPs in the SRP formulation has resulted in improvements in various properties of the SRP film.

3.4. Study on improvement of acrylic coatings' microbial ability

To enhance the longevity of organic coatings, it is crucial to address the influence of microorganisms. Effective antimicrobial properties are essential to extend the shelf life of coatings. In typical paint formulations, R-TiO₂ particles are commonly employed as pigments, known for their excellent coverage capabilities. Given the multifaceted factors affecting paint coating performance, we will focus our research on antimicrobial additives within an acrylic paint formulation that includes 2 wt % of mTi3T NPs (A2mTi3T).

3.4.1. Effect of Ag-Zn/zeolite on acrylic coatings properties

3.4.1.1. Effect of Ag-Zn/zeolite on acrylic coatings abrasion resistance

Table 3.9. Abrasion resistance of acrylic coating filled with 2 wt % mTi3T incorporation with various Ag-Zn/zeolite content

Sample	Abrasion resistance (L/mil)	Oneway ANOVA
AZe	166 ± 3.84	$F = 12.4$ $p_{value} = 2.9.10^{-5}$
A2mTi3T	187 ± 6.62	
AmT0.5Ze	179 ± 3.77	
AmT1Ze	175 ± 4.34	
AmT2Ze	169 ± 3.64	

The abrasion resistance of acrylic coating filled with 1 wt % Ag-zn/zeolite (AZe) is nearly 2 times higher than A0 coating (84 L/mil), but smaller than A2mTi3T coating (Table 3.9). When adding Ag-Zn/zeolite to A2mTi3T coating with a content of 0.5; 1 and 2 wt. % (coded as AmT0.5Ze, AmT1Ze and AmT2Ze, respectively) reduced the abrasion resistance of the coating. It proves that Ag-Zn/zeolite does not greatly affect the mechanical properties of the coating.

3.4.1.2. Effect of Ag-Zn/zeolite on acrylic acrylic antimicrobial ability

The addition of Ag-Zn/zeolite to the coating significantly enhances its antibacterial properties, effectively eliminating 99% of *E. coli* (Table 3.10) and *S. aureus* (Table 3.11) strain. However, there is no discernible difference between the AmT1Ze and AmT2Ze coatings. Therefore, the AmT1Ze coating has been chosen for further investigation.

Table 3.10. Antibacterial activity of acrylic coatings filled with 2 wt % mTi3T incorporation with various Ag-Zn/zeolite content for *E. Coli* strain

Result of bacteria array			Antibacterial activity R	Dead bacteria (%)
Incubation time	0 h	24 h		
Samples	Log (average CFU/cm ²)	Log (average CFU/cm ²)		
Control	4.00 ± 0.04	4.03 ± 0.05	-	-
A2mTi3T	4.00 ± 0.04	4.03 ± 0.05	< 0.1	0
AmT0.5Ze	4.00 ± 0.04	1.52 ± 0.05	2.51 ± 0.1	99.69
AmT1Ze	4.00 ± 0.04	0.04	3.99±0.05	99.99
AmT2Ze	4.00 ± 0.04	0.04	3.99±0.05	99.99

Table 3.11. Antibacterial activity of acrylic coatings filled with 2 wt % mTi3T incorporation with various Ag-Zn/zeolite content for *S. aureus* strain

Result of bacteria array			Antibacterial activity R	Dead bacteria (%)
Incubation time	0 h	24 h		
Samples	Log (average CFU/cm ²)	Log (average CFU/cm ²)		
Control	4.08	4.01 ± 0.05	-	-
A2mT	4.08	4.00 ± 0.05	< 0.1	2.28
AmT0.5Ze	4.08	1.72 ± 0.03	2.29±0.08	99.49
AmT1Ze	4.08	0.38 ± 0.01	3.63±0.06	99.98
AmT2Ze	4.08	0.04 ± 0.01	3.97±0.06	99.99

3.4.1.3. Effect of Ag-Zn/zeolite on thermal stability of acrylic coating

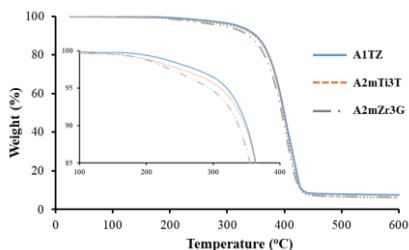


Fig. 3.26. TGA and dTGA of acrylic coating filled with various fillers

TGA diagram (Fig. 3.26) indicated that Ag-Zn/zeolite particles insignificantly affect to thermal stability of acrylic coating filled with mTi3T NPs.

3.4.1.4. Effect of Ag-Zn/zeolite on weather resistance of acrylic coating

- FTIR analysis: Based on FTIR spectrum analysis of the coating before and

after weather testing, the changes in the CI (Figure 3.27) and the PI (Figure 3.28) of the acrylic coatings have been determined. It was found that the A0 coating tended to have the largest increase in the CI but the smallest increase in PI.

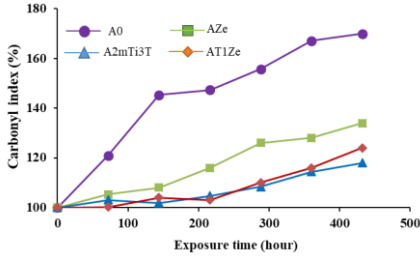


Fig. 3.27. The CI changes of acrylic coating filled with mTi3T and Ag-Zn/zeolite before and after (36 cycles - 432 hours) weathering test

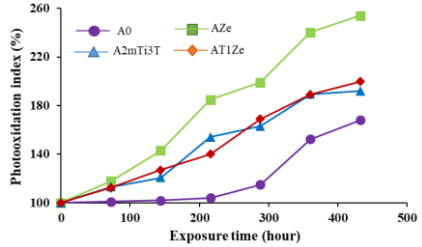


Fig. 3.28. The PI changes of acrylic coating filled with mTi3T and Ag-Zn/zeolite before and after (36 cycles - 432 hours) weathering test

- Weight loss of acrylic coating filled with mTi3T NPs and Ag-Zn/zeolite

During testing, the weight of acrylic coatings containing additives tended to increase during the first 72 hours of accelerated weathering test (Fig. 3.29). After that, the weight of these coatings tends to decrease. The reason for this difference is that the degradation mechanisms of acrylic coatings containing and without different additives are different.

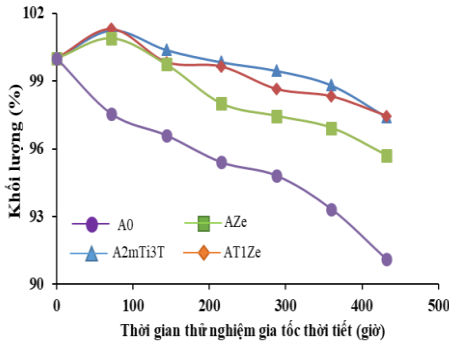


Fig. 3.29. The change of weight acrylic coating filled with Ag-Zn/zeolite and mTi3T NPs upon weathering test

Thus, Ag-Zn/zeolite particles does not enhance the properties of acrylic coating (abrasion resistance, thermal stability and weather resistance) like mTi3T NPs. However, acrylic coatings containing Ag-Zn/zeolite have good antibacterial properties. Acrylic coating containing 1% wt Ag-Zn/zeolite is capable of killing 99% of *E. coli* and *S. aureus* bacteria after 24 hours of testing

3.4.2. Study on acrylic coating filled with OIT

3.4.2.1. Effect of OIT content on antibacterial ability

OIT can inhibit the growth of microorganisms at very small concentrations

(minimum inhibitory concentration of OIT in the range of 2.5-10 ppm). Therefore, in this thesis, the OIT content is very small at 0.1, 0.2 and 0.5 wt.% to investigate the anti-microbial ability of A2mTi3T fomalur without investigating the effect of the OIT content on other properties of acrylic coating. Test results show that OIT has no antibacterial activity against two strains of bacteria *E. coli* (Table 3.12) and *S. aureus* (Table 3.13).

Table 3.12. Antibacterial activity of acrylic coatings filled with various OIT content for *E. Coli* strain

Result of bacteria array			Anti-bacterial activity R	Dead bacteria (%)
Incubation time	0 h	24 h		
Sample	Log (Average CFU/cm ²)	Log (Average CFU/cm ²)		
Control	4.00 ± 0.04	4.03	-	-
A2mTi3T/0.1wt.% OIT	4.00 ± 0.04	4.03	< 0.1	0
A2mTi3T/0.2wt.% OIT	4.00 ± 0.04	4.03	< 0.1	0
A2mTi3T/0.5wt.% OIT	4.00 ± 0.04	4.03	< 0.1	0

Table 3.13. Antibacterial activity of acrylic coatings filled with various OIT content for *S. aureus* strain

Result of bacteria array			Anti-bacterial activity R	Dead bacteria (%)
Incubation time	0 h	24 h		
Sample	Log (CFU/cm ²)	Log (CFU/cm ²)		
Control	4,08 ± 0,04	4,01 ± 0,05	-	-
A2mTi3T/0.1wt.% OIT	4,08 ± 0,04	4,01 ± 0,05	< 0,1	0
A2mTi3T/0.2wt.% OIT	4,08 ± 0,04	4,01 ± 0,05	< 0,1	0
A2mTi3T/0.5wt.% OIT	4,08 ± 0,04	4,01 ± 0,05	< 0,1	0

3.4.2.2. Effect of OIT and Ag-Zn/zeolite on mold of acrylic coating

Acrylic coating containing organically modified R-TiO₂ NPs combined with OIT has good antifungal properties. Acrylic coating using a combination of 1 wt % Ag-Zn/zeolite and 0.1 wt % OIT has the ability to synergistically enhance antibacterial and antifungal activity.

Table 3.14. Antifungal ability of acrylic coating contains different OIT content and 1 wt % Ag-Zn/zeolite

Sample	Evaluation time (day)	Percentage of surface area contaminated with fungi (%)	Antifungal level
A2mTi3T/0,1 wt.% OIT	28	0	1
A2mTi3T/0,2 wt.% OIT	28	0	0
A2mTi3T/0,5 wt.% OIT	28	0	0
AT1Ze	28	11	2b
AT1Ze/0,1 wt.% OIT	28	0	0

3.4.3. Effect of agents on antimicrobial ability of SRP

3.4.3.1. Effect of agents on light diffuse reflectance

Based on the findings (3.4.1 and 3.4.2), the combination of Ag-Zn/zeolite and OIT was chosen as the antimicrobial additive for the SRP formula (SRPK). Notably, the radiation reflection ability of SRPK is comparable to that of SRP1.

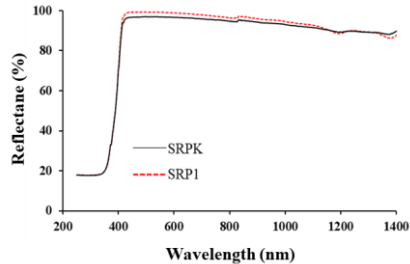


Fig. 3.30. Diffuse reflectance spectroscopy of SRP with different antibacterial agents

3.4.3.2. The antibacterial ability of solar reflective paint contains different antimicrobial additives

Observing the data in Tables 3.28 and Table 3.29, we see that after 24 hours of testing, the solar heat-reflective paint films were able to destroy most of the two tested bacterial strains, *E. coli* and *S. aureus* (> 99 %).

Table 3.15. Antibacterial activity of solar reflective paint filled with various antimicrobial agents for *E. coli* strain

Result of bacteria array			Antibacterial activity R	Dead bacteria (%)
Incubation time	0 h	24 h		
Sample	Log (CFU/cm ²)	Log (CFU/cm ²)		
Control	4.04 ± 0.04	4.06 ± 0.05	-	-
SRP1	4.04 ± 0.04	1.35 ± 0.05	2.71 ± 0.1	99.81
SRPK	4.04 ± 0.04	0.05	4.01	99.99

Table 3.16. Antibacterial activity of solar reflective paint filled with various antimicrobial agents for *S. aureus* strain

Result of bacteria array			Antibacterial activity R	Dead bacteria (%)
Incubation time	0 h	24 h		
Sample	Log (CFU/cm ²)	Log (CFU/cm ²)		
Control	4.06	4.04 ± 0.05	-	-
SRP1	4.06	0.58 ± 0.05	3.46 ± 0.1	99.96
SRPK	4.06	0.29 ± 0.04	3.75±0.09	99.98

3.4.3.3. Antifungal ability of solar reflective paint

Table 3.17. Antifungal ability of SRP containing microbial agents

Sample	Evaluation time (day)	Percentage of surface area contaminated with fungi (%)	Antifungal level
SRP1	28	0	1
SRPK	28	0	0

Thus, the solar reflective paint containing the antimicrobial additive Ag-Zn/zeolite combined with OIT has good antibacterial ability against two tested bacterial strains (*E. coli* and *S. aureus*) and better fungal resistance than commercial antibacterial additives commonly used for water-based paints. On the other hand, Ag-Zn/zeolite and OIT do not greatly affect the ability of the paint to reflect light.

CONCLUSION

1. The suitable organic agents for the modification of R-TiO₂ and ZrO₂ NPs are [3-(methacryloyloxy)propyl]trimethoxysilane (TMSPM) and (3-glycidyloxypropyl)triethoxysilane (GPTES), respectively, each with an appropriate initial content of 3 wt.% (compared to NPs content). The content of TMSPM and GPTES grafted on R-TiO₂ and ZrO₂ NPs is 0.122 mmol/g (29.8 mg/g) and 0.068 mmol/g (18.9 mg/g). Organic modification enhances NPs' light diffuse reflectance and dispersion into acrylic emulsion polymer, while exhibiting insignificant influence on morphology and crystalline structure.

2. The suitable content for incorporating the above organically modified NPs into the emulsion acrylic nanocomposite coating, referred to as the acrylic coating film, is 2 wt%. In comparison to acrylic coatings filled with only a single type of NPs, acrylic coatings containing a blend of the aforementioned NPs (at weight ratio of 1:1) exhibit enhanced properties. These include superior weather resistance and 10% improvement of abrasion resistance. Additionally,

the decomposition onset temperature increases by more than 10°C, and the radiation reflection capability improves by 20%.

3. The SRP integrates a mixture of R-TiO₂ and ZrO₂ NPs (at a 1:1 weight ratio), replacing 1% of R-TiO₂ microparticles. This modification markedly improves the SRP's capacity to reflect diffuse radiation, resulting in an approximate 5% increase compared to SRP films without NPs. Furthermore, it significantly reduces water penetration by up to 50%, enhancing waterproofing properties. Additionally, the SRP film improves cooling performance, reducing the surface temperature by around 4°C compared to films without NPs.

4. The addition of Ag-Zn/zeolite to acrylic coatings has a minimal impact on overall properties but significantly boosts the antibacterial effectiveness. In contrast, 2-n-octyl-4-isothiazolin-3-one (OIT) lacks antibacterial efficacy against *E. coli* and *S. aureus*; however, it excels in mold resistance. The combined antimicrobial system of Ag-Zn/zeolite and OIT maintains the paint film's reflective and diffusive radiation abilities. Notably, it demonstrates potent antimicrobial action, eliminating over 99% of *E. coli* and *S. aureus* bacteria (with an initial density of $\sim 10^4$ CFU/cm²) and effectively preventing fungal growth after 28 days.

NOVELTY CONTRIBUTIONS OF THE THESIS

1. The thesis has put forth suitable conditions for the modification of R-TiO₂ and ZrO₂ NPs using the respective agents [3-(methacryloyloxy)propyl]-trimethoxysilane (TMSPM) and (3-glycidyloxypropyl)triethoxysilane (GPTES). These modifications aim to enhance the compatibility and dispersion of the NPs within the acrylic emulsion polymer and thus contributing improvement of the coating's properties.

2. The thesis has demonstrated a synergistic effect through the combination of modified NPs with antibacterial agents Ag-Zn/zeolite and 2-n-octyl-4-isothiazolin-3-one (OIT). This combination serves to simultaneously enhance various features of the water-based acrylic coating, including mechanical properties, thermal stability, the ability to reflect solar radiation, as well as antibacterial and antifungal characteristics.

3. The thesis has made a significant contribution to the field by developing environmentally friendly water-based paint. This innovative paint formulation not only possesses the capability to reflect solar heat but also demonstrates resistance to microorganisms. These advancements make it a promising solution for application in construction projects, contributing to both sustainability and improved performance in built environments.

LIST OF THE PUBLICATIONS RELATED TO THE DISSERTATION

1. **Phi Hung Dao**, Thuy Chinh Nguyen, Thi Lan Phung, Tien Dung Nguyen, Anh Hiep Nguyen, Thi Ngoc Lan Vu, Quoc Trung Vu, Dinh Hieu Vu, Thi Kim Ngan Tran, and Hoang Thai - Assessment of Some Characteristics and Properties of Zirconium Dioxide NPs Modified with 3-(Trimethoxysilyl) Propyl Methacrylate Silane Coupling Agent - Journal of Chemistry, Volume 2021, Article ID 9925355, 10 pages (SCIE – IF: 3,241).

2. **Phi Hung Dao**, Tien Dung Nguyen, Thuy Chinh Nguyen, Anh Hiep Nguyen, Van Phuc Mac, Huu Trung Tran, Thi Lan Phung, Quoc Trung Vu, Dinh Hieu Vu, Thi Cam Quyen Ngo, Manh Cuong Vu, Vu Giang Nguyen, Dai Lam Tran, Hoang Thai - Assessment of some characteristics, properties of a novel waterborne acrylic coating incorporated TiO₂ NPs modified with silane coupling agent and Ag/Zn zeolite - Progress in Organic Coatings 163 (2022) 106641 (SCIE – IF: 6,13)

3. Thuy Chinh Nguyen, **Phi Hung Dao**, Quoc Trung Vu, Anh Hiep Nguyen, Xuan Thai Nguyen, Thi Ngoc Lien Ly, Thi Kim Ngan Tran, Hoang Thai - Assessment of characteristics and weather stability of acrylic coating containing surface modified zirconia NPs - Progress in Organic Coatings 163 (2022) 106675 (SCIE – IF: 6,13).

4. **Phi Hung Dao**, Thi Lan Phung, Anh Hiep Nguyen, Van Phuc Mac, Xuan Thai Nguyen, Thuy Chinh Nguyen, Quoc Trung Vu, Thi My Binh Dinh, Hoang Thai - Effect of organically modified titania and zirconia NPs on characteristics, properties of coating based on acrylic emulsion polymer for outdoor applications – Journal of Applied Polymer Science, 140 (16) (2023), e53752 (SCIE – IF: 3,125).

5. Nguyen Thuy Chinh, Tran Thi Mai, **Dao Phi Hung**, Nguyen Anh Hiep, Nguyen Thi Thu Trang, Tran Huu Trung, Nguyen Xuan Thai, Dao Huu Toan, Dinh Thi My Binh, Thai Hoang - Characteristics of organic titanate modified titanium dioxide NPs and its dispersibility in acrylic emulsion coating - Vietnam J. Chem., 2022, 60 (special issue), 116-124 (DOI: 10.1002/vjch.202200080) (Scopus, IF = 0,9, Q3).

6. Nguyen Thuy Chinh, **Dao Phi Hung**, Nguyen Xuan Thai, Nguyen Anh Hiep, Thai Hoang – Assessment of influence of modified zirconia NPs content on the weather resistance of acrylic coating – Vietnam Journal of Science and Technology, 61(5) (2023) 844-853 (doi:10.15625/2525-2518/16686) (Scopus, Q4).

7. **Sáng chế số 35923**: Thái Hoàng, **Đào Phi Hùng**, Nguyễn Thúy Chinh, Nguyễn Anh Hiệp, Trần Đại Lâm, Vũ Quốc Trung, Đinh Thị Mỹ Bình – Phương pháp sản xuất hệ sơn phủ lai hữu cơ – vô cơ và hệ sơn thu được từ phương pháp trên có khả năng chống nóng, bền mài mòn và kháng khuẩn (Được cấp bằng theo Quyết định 26122/QĐ-SHTT.IP ngày 04/5/2023).